

## Application of spherical $\text{Ni}(\text{OH})_2$ /CNTs composite electrode in asymmetric supercapacitor

WANG Xiao-feng(王晓峰), RUAN Dian-bo(阮殿波), YOU Zheng(尤 政)

Department of Precision Instruments and Mechanology, Tsinghua University, Beijing 100084, China

Received 6 December 2005; accepted 8 May 2006

**Abstract:** The composite electrodes consisting of carbon nanotubes and spherical  $\text{Ni}(\text{OH})_2$  are developed by mixing nickel hydroxide, carbon nanotubes and carbonyl nickel powder together in 8:1:1 ratio. A maximum capacitance of 311 F/g is obtained for an electrode prepared with the precipitation process. In order to enhance energy density, an asymmetric type pseudo-capacitor/electric double layer capacitor is considered and its electrochemical properties are investigated. Values for the specific energy and maximum specific power of 25.8 W·h/kg and 2.8 kW/kg, respectively, are demonstrated for a cell voltage between 0 and 1.6 V. By using the modified cathode of a  $\text{Ni}(\text{OH})_2$ /carbon nanotube composite electrode, the asymmetric supercapacitor exhibits high energy density and stable power characteristics.

**Key words:** nickel hydroxide; carbon nanotubes; activated carbon; asymmetric supercapacitor

### 1 Introduction

Electrochemical capacitors (hereafter ECs) have greater power density than usual batteries and can be deeply discharged without any deleterious effect on life time[1]. Activated carbon(AC) with various modifications is the electrode material used most frequently for electrodes of ECs. Carbons are available with a specific surface area of up to 2 500 m<sup>2</sup>/g as powders, woven cloths, felts, or fibers[2]. Charge storage on carbon electrodes is predominantly capacitive in the electrochemical double layer. Carbon based ECs come close to what one would call an electrochemical double layer capacitor(EDLC).

Amorphous ruthenium oxide is considered to be a promising material for a high energy density power source because the charge can be stored in the bulk amorphous materials[3]. However, the high material cost of  $\text{RuO}_2 \cdot x\text{H}_2\text{O}$  makes this material inadequate for commercial applications[4]. Therefore, in recent years, great efforts were taken in order to find new and cheaper materials. There are also other approaches, e.g. polymers [5], nitrides[6, 7] and manganese oxides[8]. Sol-gel derived  $\text{Ni}_x\text{O}/\text{Ni}$  thin film electrodes or nickel oxides prepared in electrochemical route calcined at 300 °C provide a specific capacitance of 200 to 260 F/g[9,10].

CONWAY[11] reported that  $\text{Co}_3\text{O}_4$  and  $\text{CoO}_x$  are promising electrode materials for ECs due to their intercalative pseudo-capacitance properties. LIU et al's study [12] shows that cobalt oxide films exhibit pseudo-capacitance behavior in the potential range of -2 V to -1.56 V at the sweep rate of 20 mV/s. LIN et al[13] investigated the redox behavior and charging mechanism of an electrode prepared with  $\text{CoO}_x$  xerogel calcined at 150 °C and a maximum capacitance of 291 F/g was obtained. These materials show high pseudocapacitance and good electronic conductivity. However, the technique applied in these literatures is too sophisticated to be used in practical situations. The difference between potentials of discharged electrode and charged electrode is not significant (about 400 mV for nickel and 600 mV for cobalt) in contrast to  $\text{RuO}_x$  capacitors possessing wide window of potentials (more than 1 000 mV). So the performance of "pure" pseudocapacious systems based on nickel or cobalt oxide is poor.

Carbon nanotubes(CNTs) were discovered in 1991. Their high accessible surface area, low resistance and high stability suggest that CNTs are suitable materials for electrodes in ECs[14,15]. We report here the composite of nickel hydroxide and CNTs for ECs with high capacitance and low resistance. The electrochemical activity of nickel hydroxide is improved by the introduction of CNTs matrix in the hydroxide.

Asymmetric supercapacitors using an EDLC-pseudocapacitor to increase energy density were introduced by BELIAKOV et al[16]. The term "Asymmetric" means that this capacitor employs asymmetric electrodes with different operating voltage windows. These asymmetric electrodes are responsible for the ability to achieve an operating voltage over 1.2 V even in aqueous electrolyte. Wide operating voltage yields high energy density. If one of the electrodes of the cell was not polarizable, or partially polarizable when the potential of the other electrode was changed, it could lead to a doubling of the electrical capacitance of the cell. In this paper, we propose a new asymmetric supercapacitor consisting of spherical nickel hydroxide composite as cathode, activated carbon as anode, and 6 mol/L KOH as the electrolyte. The maximum energy density and power density of the ECs are both modified in this way.

## 2 Experimental

### 2.1 Preparation of $\text{Ni}(\text{OH})_2$ and carbon nanotubes electrode material for supercapacitor

Carbon nanotubes were produced catalytically with Ni particles as the catalyst[17]. In a pipe stove, with reagent based on Ni and ethylene gas, multi-walled carbon nanotubes were produced at 700 °C. Scanning electron micrograph(SEM) of carbon nanotubes after nitric acid treatment is shown in Fig.1. The nanotubes have a diameter of 15–50 nm and length of several microns to several tens of microns.

The nickel hydroxide was prepared in a process as discussed in Refs.[18, 19]. A nickel sulfate solution and ammonium hydroxide were continuously mixed in a premixing vessel to form a nickel ammonium complex, and then the mixed solution and a sodium hydroxide solution were continuously supplied to a reactor. 0.5 mol/L nickel sulfate solution and 15 mol/L ammonium hydroxide in a ratio of 0.8 mol ammonia to 1.0 mol nickel ion were continuously mixed in a premixing vessel at 50 °C. The mixed solution and 6.0 mol/L sodium hydroxide solution were then continuously fed in a reactor at 50 °C, while maintaining the pH value at 11 with a variation of  $\pm 0.1$ . Nickel hydroxide was produced using a residence time of 6 h to control the particle size. The SEM morphology of spherical  $\text{Ni}(\text{OH})_2$  prepared is shown in Fig.2. The spherical particles have a diameter of 1–20  $\mu\text{m}$ .

### 2.2 Preparation of electrode and assemble of asymmetric supercapacitor

Polarizable capacitor electrodes can be manufactured using  $\text{Ni}(\text{OH})_2/\text{CNTs}$  according to the invention of conventional method well known[19]. For

the preparation of the  $\text{Ni}(\text{OH})_2/\text{CNTs}$  composite electrode, the designed amount of CNTs and conductive agent (carbonyl nickel powders) were mixed physically in  $\text{Ni}(\text{OH})_2$ . Thus, the electrode materials were mixed with polytetrafluoroethylene (PTFE) and dispersed in isopropyl alcohol solution. The mixing ratio of  $\text{Ni}(\text{OH})_2$  to CNTs to carbonyl nickel was 8:1:1 and we controlled PTFE at 5% (mass fraction) vs the total mass of electrode materials. The paste-like mixture obtained was then rolled to form flexible films with a thickness of 0.2 mm. This film-like raw material for electrodes was cut into electrode with preferred size and shape. The electrodes were then mounted on a porous Ni plaque-current collector. They were dried again under vacuum at 100 °C for 24 h. Composites with 10% CNTs and 10% carbonyl nickel were prepared with this technique. As anodes, pure activated carbon(AC, YP-15, Klordi, Japan)-based electrodes were prepared by the same method.

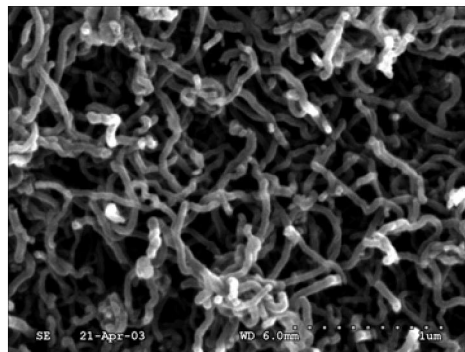


Fig.1 SEM morphology of carbon naotubes

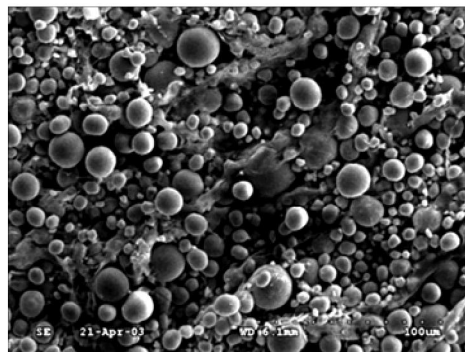


Fig.2 SEM morphology of  $\text{Ni}(\text{OH})_2$  particles

### 2.3 Electrochemical test of performance for composite electrodes and asymmetric supercapacitor

Two tested cells were introduced in this paper. A beaker-type electrochemical cell equipped with a working electrode, a platinum counter electrode and SCE reference electrode were used. The electrodes were simply dipped into 6 mol/L KOH. The geometric surface area of the working electrode was 1  $\text{cm}^2$  and the mass

was 7.5 mg. The cyclic voltammograms presented in this paper were steady state ones after repeated potential sweeps. The electrochemically active surface area includes both the charge of the electrical double layer and that of the redox of the metal species, i.e., it reflects the pseudo-capacitance of the electrodes. They were connected to CHI 660B system that drove the voltage in either direction sequentially at predetermined constant sweep rates. The sweep rate range of  $20 \text{ mV} \cdot \text{s}^{-1}$  was used during testing.

Another cell has much more characteristic of an actual working device. The  $\text{Ni}(\text{OH})_2/\text{CNTs}$  cathode and AC anode were pressed together and separated by a porous non-woven cloth separator. The mass ratio of active materials(cathode/anode) was 0.5 g:0.4 g. The geometric surface area of both electrodes was  $10 \text{ cm}^2$ . The dc charge/discharge test was performed to evaluate the electrochemical performance of the combined capacitor with a current density from  $10 \text{ mA/cm}^2$  to  $50 \text{ mA/cm}^2$ . All the above electrochemical measurement was carried out on CHI660B.

The specific capacitance of the asymmetric capacitor can be evaluated from the charge/discharge test together with the following equation:

$$C = \frac{I \Delta t}{\Delta V} \quad (1)$$

where  $C$  is the capacitance, F;  $I$  is the discharge current, A;  $\Delta t$  is the time period(s) for the potential change  $\Delta V$ , V. By comparing the linearity of the voltage change with respect to time during the discharge period, the capacitance  $C$  was calculated by the potential change from 0 to 1.6 V.

The real power density  $P_{\text{real}}$  is determined from the constant current charge/discharge cycles as follows [20, 21, 22]:

$$P_{\text{real}}/(\text{W} \cdot \text{g}^{-1}) = \Delta E \cdot I/m \quad (2)$$

where  $\Delta E = (E_{\text{max}} + E_{\text{min}})/2$  with  $E_{\text{max}}$  as the potential at the beginning of discharge and  $E_{\text{min}}$  at the end of discharge,  $I$  is the applied current(A), and  $m$  is the mass of active material in the electrodes(g).

Alternatively, the maximum specific power,  $P_{\text{max}}$ , is calculated from

$$P_{\text{max}}/(\text{W} \cdot \text{g}^{-1}) = U_0^2 / 4Rm \quad (3)$$

where  $U_0$  is the potential at the end of charge and  $R$  is the equivalent serials resistance ( $\Omega$ ).

The real specific energy  $E_{\text{real}}$  is defined as

$$E_{\text{real}}/(\text{W} \cdot \text{g}^{-1}) = \frac{C(U_{\text{max}})^2}{2m} \quad (4)$$

where  $C$  is the system capacitance(F) for a cell and  $U_{\text{max}}$  is the potential at the beginning of discharge.

The maximum specific energy  $E_{\text{max}}$  is defined as

$$E_{\text{max}}/(\text{J} \cdot \text{g}^{-1}) = \frac{C(U_0)^2}{2m} \quad (5)$$

where  $C$  is the system capacitance (F) for a cell and  $U_0$  is the potential at the end of charge.

### 3 Results and discussion

#### 3.1 Pseudocapacitance of $\text{Ni}(\text{OH})_2/\text{CNTs}$ composite electrode

A cyclic voltammetric(CV) measurement is helpful to understanding the macroscopic electrochemical surface reactions at the electrode of the supercapacitor during the charging and discharging process. Cyclic voltammograms on the pure  $\text{Ni}(\text{OH})_2$  and  $\text{Ni}(\text{OH})_2/\text{CNTs}$  composite electrodes are performed to investigate the possible dominant mode of electrochemical energy storage on the three electrodes. Fig.3 presents the cyclic voltammetric behaviors of  $\text{Ni}(\text{OH})_2$  (Fig.3(a)), and  $\text{Ni}(\text{OH})_2/\text{CNTs}$  (Fig.3(b)) electrodes at a sweep rate of  $20 \text{ mV/s}$ . The  $\text{Ni}(\text{OH})_2$  electrode clearly shows faradaic redox reactions, which are observed at 0.3 V and 0 V with respect to the SCE reference electrode representing oxidation and reduction processes. The  $\text{Ni}(\text{OH})_2/\text{CNTs}$  electrode shows a shape similar to that of the  $\text{Ni}(\text{OH})_2$  electrode basically, having the faradaic redox behavior. However, the usable potential window of composite electrode is much wider than that of the  $\text{Ni}(\text{OH})_2$  electrode. Redox peak behaviors are observed at a wide range of voltage. The  $\text{Ni}(\text{OH})_2/\text{CNTs}$  composite electrode shows faradaic redox reactions representing oxidation and reduction processes at 0.3 V and  $-0.2 \text{ V}$ , respectively. Consequently, the electrochemical capacitance scale of composite is much larger than that

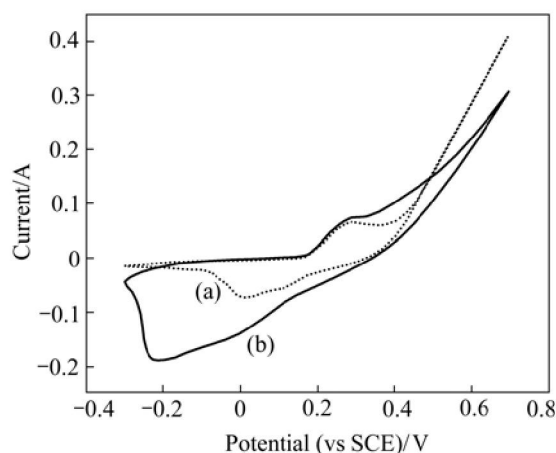


Fig.3 Cyclic voltammogram for electrode at scanning rate of  $20 \text{ mV/s}$  in  $6 \text{ mol/L KOH}$ : (a)  $\text{Ni}(\text{OH})_2$ ; (b)  $\text{Ni}(\text{OH})_2/\text{CNTs}$

of the individual materials. From integrating the CV curve, the  $\text{Ni}(\text{OH})_2/\text{CNTs}$  composite electrode shows about 311 F/g specific capacitance as a single electrode capacitance; while the capacitance of the  $\text{Ni}(\text{OH})_2$  electrode is no more than 137 F/g.

We can see from the CV curves that the  $\text{Ni}(\text{OH})_2/\text{CNTs}$  composite electrode shows the characteristics of a pseudo-capacitive electrode. This wider potential scope for the  $\text{Ni}(\text{OH})_2/\text{CNTs}$  composite electrode results from the uniform mixture of  $\text{Ni}(\text{OH})_2$  with CNTs, which increases effectively the active sites on the hydroxide particles. The effective surface area of the  $\text{Ni}(\text{OH})_2$  surrounded by CNTs is enhanced distinctly in the composite in comparison to the pure  $\text{Ni}(\text{OH})_2$  electrode, as mentioned previously. Two different roles of carbon additives can be expected. One is as an electrolyte reservoir to reduce ionic diffusion resistance regardless of charging/discharging current density, as shown in Fig.4. This is caused by the high specific surface area ( $A_{\text{BET}}$ ) of about 500  $\text{m}^2/\text{g}$ . At the same time, a large surface area of CNTs would contribute to the charge storage by the EDLC mechanism[23].

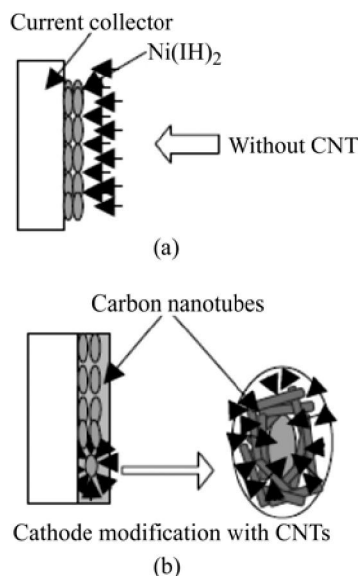


Fig.4 Schematic diagram of electrode structure

The activated carbon (AC YP-15) was provided by Klordi (Japan). Cyclic voltammeteries on the AC electrodes are performed to investigate the capacitance of the active material. The curve (b) in Fig.5 shows the CV curve of the AC-based electrode in the KOH electrolyte at scanning rate of 20 mV/s. The charging and discharging cyclic voltammogram CV is close to a rectangular shape, indicating a typical electric double layer EDLC behavior because no peaks of oxidation and reduction are observed. From integrating the CV curve, the AC electrode shows about 156 F/g specific capacitance as a single electrode capacitance.

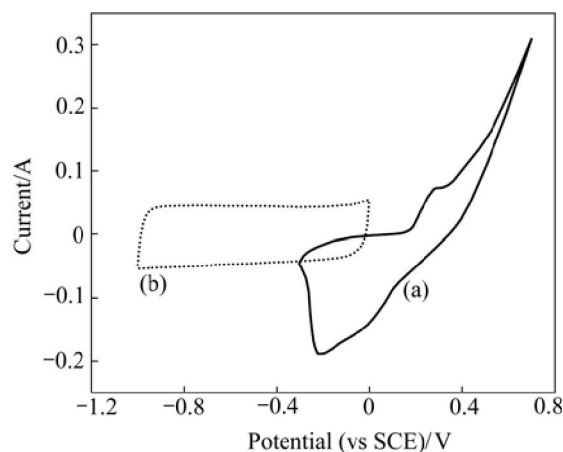


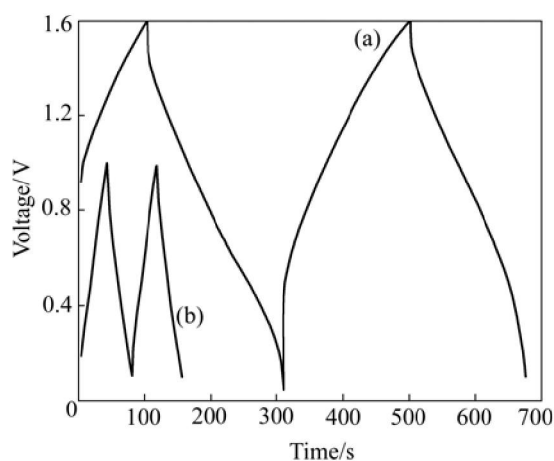
Fig.5 Cyclic voltammogram for cathode and anode in asymmetric supercapacitor: (a)  $\text{Ni}(\text{OH})_2/\text{CNTs}$  cathode; (b) AC anode

### 3.2 Electrochemical performance of asymmetric supercapacitor

In contradistinction to  $\text{RuO}_x$  capacitors possessing wide window of potentials in anode and cathode areas, the difference between potentials of discharged electrode,  $\text{Ni}(\text{OH})_2$ , and charged electrode,  $\text{NiOOH}$ , is not significant (about 100–400 mV) according to Fig.3. Thus, it's not expedient to create "pure" pseudocapacitive systems, such as  $[\text{+NiOOH/KOH/Ni}(\text{OH})_2\text{-}]$ . Therefore, in order to widen the working voltage window, AC-based material has been adapted to an anode[24]. This electrochemical system can be written as follows:  $[\text{+NiOOH/KOH/AC-}]$ . The principle of charge of  $\text{Ni}(\text{OH})_2$  is based on transferring of charge throughout the interface of phase. During the process of charge of carbon anode, a double electric layer is created. The electrodes included into the system are notable for their reversibility. The process of discharge for this new type super-capacitor is a process of portonization of crystal grid  $\text{NiOOH}$  and destruction of layer of hydrated ions on an activated carbon electrode. We can also expect that replacement of the anode electrode from  $\text{Ni}(\text{OH})_2/\text{CNTs}$  to AC contributes to improving the energy density of ECs. Furthermore, the AC-based anode that has the power characteristics of EDLC would contribute to improving the power characteristics of the asymmetric supercapacitor in this study.

In order to get information about the ability of the  $\text{Ni}(\text{OH})_2/\text{CNTs}$  composite as an electrode material of cathode in the asymmetric supercapacitor mentioned above, constant charge/discharge cycles are realized in aqueous media with 6 mol/L KOH as a supporting electrolyte. Fig.6 shows the constant current charge/discharge curve of a unit capacitor cell fabricated with a  $\text{Ni}(\text{OH})_2/\text{CNTs}$  composite electrode as a cathode and activated carbon electrode as an anode. The cutoff

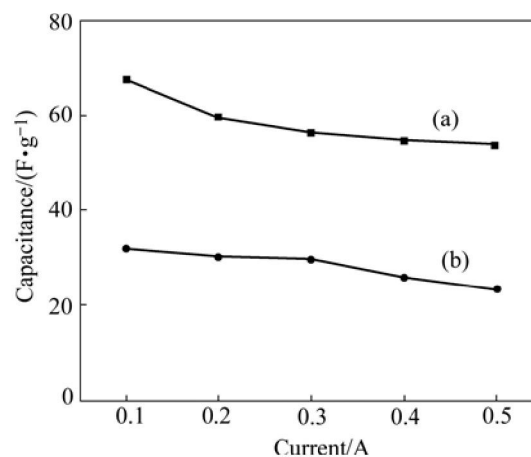
voltage of charging/discharging is 0–1.6 V with 0.1–0.5 A current at room temperature. The activated carbon electrode used as anode is cycled without significant damage to the CV curves between –1 and 0 V (vs SCE) and the composite electrode used as cathode shows stable CV characteristics between –0.3 and 0.6 V (vs SCE). Thus, a pseudocapacitor/EDLC asymmetric supercapacitor is cycled galvanostatically at 1.6 V of upper cut-off voltage. Before the charge/discharge test, each cell is treated potentiostatically for aging of each electrode. During the charging and discharging steps, though an almost linear variation of the cell voltage is observed (a), perfect linear curves are not obtained compared with the case of EDLC. This is due to the nonlinear redox process occurring at the cathode electrode during charging and discharging. In comparison with the asymmetric capacitor, we fabricate a two-electrode AC-based symmetric capacitor and it is cycled galvanostatically between 0 and 1.0 V. It shows an ideal EDLC behavior by a linear charge/discharge behavior (b).



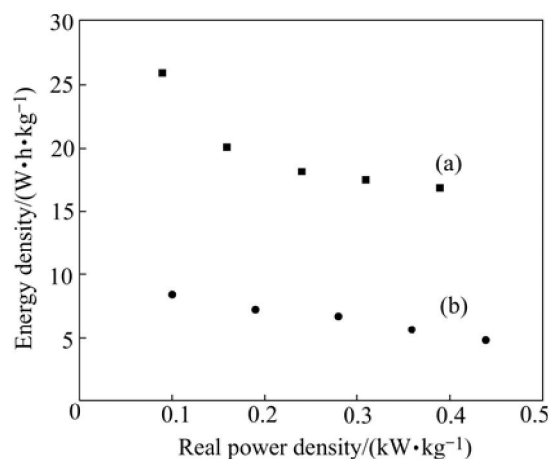
**Fig.6** Voltage profile of a charge/discharge cycle of EDLC and asymmetric super capacitor at 0.2 A: (a) Asymmetric capacitor; (b) EDLC capacitor

Fig.7 shows the specific capacitance of the double electrode cell as a function of charge/discharge current for the composite electrode-based asymmetric supercapacitor (cathode: composite electrode, anode: activated carbon) and the AC based EDLC. Although the capacitance of the activated carbon is lower compared with the pseudocapacitance of the  $\text{Ni}(\text{OH})_2$ , the AC-based EDLC shows better power characteristics between 0.1 A and 0.5 A. From Fig.7, it is known that the specific capacitance of a unit cell is enhanced by using  $\text{Ni}(\text{OH})_2/\text{CNTs}$  composite as cathode. For the asymmetric supercapacitor, the maximum specific capacitance of 68 F/g is obtained by dividing the unit cell capacitance by the total mass of cathode and anode active materials (active material+binder+conducting

agent). The value is more than 2 times that obtained from the AC-based EDLC. On the other hand, we can see that the power characteristics of the asymmetric cell are decreased slightly with increasing of discharging current density especially at low discharge current. The faradic reactions cause salt starvation around  $\text{Ni}(\text{OH})_2$  particles resulted from adsorption of a large amount of  $\text{H}^+$  ions at high current density. The real specific power  $P_{\text{real}}$  and real energy density  $E_{\text{real}}$  for the asymmetric supercapacitor and AC based EDLC are shown in Fig.8. The energy and power data are calculated when taking account of only the mass of the electrode material. The energy density of asymmetric supercapacitor increases from 16.8 W·h/kg to 25.8 W·h/kg when the real power density decreases from 0.4 kW/kg to 0.1 kW/kg. The maximum specific power density  $P_{\text{max}}$  reaches the value of 2.8 kW/kg according to the equation (3). The specific energy increases by more than 4 times compared with that of a symmetric AC-based EDLC capacitor using an aqueous KOH electrolyte.



**Fig.7** Specific capacitance for asymmetric supercapacitor and AC-based EDLC capacitor: (a) Asymmetric capacitor; (b) EDLC capacitor



**Fig.8** Power and energy density for asymmetric supercapacitor and AC-based EDLC capacitor: (a) Asymmetric capacitor; (b) EDLC capacitor

## 4 Conclusions

The nickel hydroxide  $\text{Ni}(\text{OH})_2$  with high capacitance due to proton exchange is examined to determine the possibility of application as a cathode material of ECs. When CNTs with high surface area and electric conductance are added to the cathode materials of  $\text{Ni}(\text{OH})_2$ , the capacitance of the electrode is improved. The introduction of CNTs in metal oxide increases the capacitance by reducing the internal resistance of the electrode. We also introduce a new asymmetric capacitor with high operating voltage, high energy density and high power density. The maximum energy density and specific power densities of the cell reach 25.8 W·h/kg and 2.8 kW/kg respectively. It should also be noted that the asymmetric capacitor delivers high power without profound loss in energy.

## References

- [1] CONWAY B E. Transition from "Supercapacitor" to "Battery" behavior in electrochemical energy storage [J]. *Journal of the Electrochemical Society*, 1991, 138(6): 1539–1544.
- [2] HUGGINS R A. Supercapacitors and electrochemical pulse sources [J]. *Solid State Ionics*, 2000, 134(1–2): 179–195.
- [3] ZHENG J P, JOW T R. A new charge storage mechanism for electrochemical capacitors [J]. *Journal of the Electrochemical Society*, 1995, 142(1): L6–L8.
- [4] ZHENG J P, JOW T R. High energy and high power density electrochemical capacitors [J]. *J Power Sources*, 1996, 62(2): 155–159.
- [5] IZADI-NAJAFABADI A, TAN D T H, MADDEN J D. Towards high power polypyrrole/carbon capacitors (Part 1) [J]. *Synthetic Metals*, 2005, 152: 129–132.
- [6] LIU T C, PELL W G, CONWAY B E. Behavior of molybdenum nitrides as materials for electrochemical capacitors—comparison with ruthenium oxide [J]. *Journal of the Electrochemical Society*, 1998, 145: 1882–1888.
- [7] DENG C Z, TSAI K C. Improved porous mixture of molybdenum nitride and tantalum oxide as a charge storage materials [J]. *Journal of the Electrochemical Society*, 1998, 145(4): L61–L64.
- [8] JIANG J H, KUCERNAK A. Electrochemical supercapacitor material based on manganese oxide: preparation and characterization [J]. *Electrochimica Acta*, 2002, 47(15): 2381–2386.
- [9] LIU K C, ANDERSON M A. Porous nickel oxide/nickel films for electrochemical capacitors [J]. *Journal of the Electrochemical Society*, 1996, 143(1): 124–130.
- [10] SRINIVASAN V, WEIDNER J W. Studies on the capacitance of nickel oxide films: Effect of heating temperature and electrolyte concentration [J]. *Journal of the Electrochemical Society*, 2000, 147(3): 880–885.
- [11] CONWAY B E. *Electrochemical Supercapacitors: Scientific Fundamentals and Technological Applications* [M]. New York: Kluwer Academic/Plenum Press, 1999.
- [12] LIU T C, PELL W G, CONWAY B E. Stages in the development of thick cobalt oxide films exhibiting reversible redox behavior and pseudocapacitance [J]. *Electrochimica Acta*, 1999, 44(17): 2829–2842.
- [13] LIN C, RITTER J A, POPOV B N. Characterization of sol-gel-derived cobalt oxide xerogels as electrochemical capacitors [J]. *Journal of the Electrochemical Society*, 1998, 145(12): 4097–4103.
- [14] WANG Xiao-feng, RUAN Dian-bo, YOU Zheng. Performance of a 60 F carbon nanotubes-based supercapacitor for hybrid power sources [J]. *Journal of University of Science and Technology Beijing*, 2005, 12: 267–273.
- [15] WANG Xiao-feng. The performance of 600F power super capacitor using carbon nanotubes electrodes and nanoaqueous electrolyte [J]. *Chinese Journal of Electronics*, 2005, 14: 45–48.
- [16] BELIAKOV A I, BRINTSEV A M. Development and application of combined capacitors: double electric layer–pseudocapacity [A]. *Proceedings of the 7th International Seminar on Double Layer Capacitors and Similar Energy Storage Devices* [C]. Deerfield Beach, Florida, USA, 1997.
- [17] JIA Z J, WANG Z Y, LIANG J, WEI B Q, WU D H. Production of short multi-walled carbon nanotubes [J]. *Carbon*, 1999, 37(6): 903–906.
- [18] BERNDT D. *Maintenance-Free Batteries—A Handbook of Battery Technology* [M]. England, Research Studies Press Ltd, 1997.
- [19] SHIN D Y. Method for Preparing High Density Nickel Hydroxide Used for Alkali Rechargeable Batteries [P]. US5498403, 1996.
- [20] BROUSSE T, TOUPIN M, BELANGER D. A hybrid activated carbon-manganese dioxide capacitor using a mild aqueous electrolyte [J]. *Journal of the Electrochemical Society*, 2004, 151(4): A614–A622.
- [21] BROUSSE T, BELANGER D. A hybrid  $\text{Fe}_3\text{O}_4$ - $\text{MnO}_2$  capacitor in mild aqueous electrolyte [J]. *Electrochemical and Solid State Letters*, 2003, 6(11): A244–A248.
- [22] HONG M S, LEE S, KIM S W. Use of KCl aqueous electrolyte for 2V manganese oxide/activated carbon hybrid capacitor [J]. *Electrochemical and Solid State Letters*, 2002, 5(10): A227–A230.
- [23] PARK J H, PARK O O, SHIN K H, JIN C S, KIM J H. An electrochemical capacitor based on a  $\text{Ni}(\text{OH})_2$ /activated carbon composite electrode [J]. *Electrochemical and Solid-State Letter*, 2002, 5(2): H7–H10.
- [24] WANG Xiao-feng, WANG Da-zhi, LIANG Ji. Pseudo-capacitance of ultrafine nickel hydroxide prepared by sol-gel method [J]. *Acta Physico-Chimica Sinica*, 2005, 21(2): 117–122.

(Edited by YANG Bing)